Published for SISSA by Springer

Received: July 27, 2026
Revised: September 30, 2026
Accepted: October 2, 2026
Published: November 2, 2026

Migdal ionization as a probe of light dark matter from nuclear transition

Yuanchao Lou,[a] **Liangliang Su**[b] **and Lei Wu**[a,c]

[a] *Department of Physics and Institute of Theoretical Physics, Nanjing Normal University, Nanjing, 210023, China*
[b] *Institute for Astroparticle Physics, Karlsruhe Institute of Technology, D-76131 Karlsruhe, Germany*
[c] *Nanjing Key Laboratory of Particle Physics and Astrophysics, Nanjing, 210023, China*

E-mail: yuanchao_lou@nnu.edu.cn, liangliang.su@kit.edu, leiwu@njnu.edu.cn

Abstract: Nuclear reactors serve as a key artificial source of light dark matter. Direct detection of reactor-produced dark matter faces substantial obstacles, since quenching effects suppress conventional elastic scattering signals below detector thresholds. We present a new search strategy utilizing the Migdal effect in germanium detectors to probe light dark matter produced via nuclear de-excitation from reactors. Using ON-OFF residual spectra from the TEXONO experiment, we set a new stringent limit on the dark matter and nucleus interaction over the mass range $0.01\,\mathrm{MeV} \leq m_\chi \lesssim 2.6\,\mathrm{MeV}$, which provides a complementary bound to existing cosmological and astrophysical limits.

Keywords: Models for Dark Matter, New Gauge Interactions, New Light Particles

ArXiv ePrint: 2607.10716

Open Access, © The Authors.
Article funded by SCOAP^3.

https://doi.org/10.1007/JHEP11(2026)014

JHEP11(2026)014

Contents

1 **Introduction** 1

2 **Dark matter production** 2

3 **Migdal signal and TEXONO limits** 4

4 **Conclusion** 7

JHEP11(2026)014

1 Introduction

The existence of dark matter (DM) is firmly established by overwhelming gravitational evidence on astrophysical and cosmological scales. However, its fundamental nature at the microscopic level remains one of the most profound mysteries in physics. For decades, the search has been dominated by the Weakly Interacting Massive Particle (WIMP) paradigm (see recent reviews, e.g. [1, 2]). Yet, the continued absence of a confirmed signal in conventional WIMP searches [3–5] has motivated a significant shift in the field towards exploring lighter DM candidates [6–18]. This poses a significant challenge for direct detection, as the resulting nuclear recoils fall far below current detector thresholds, necessitating novel detection strategies (see examples, e.g. [19–32]).

The Migdal effect provides a viable mechanism to circumvent this limitation. During a DM-nucleus scattering event, the sudden acceleration of the nucleus can lead to the ionization or excitation of atomic electrons [33, 34]. This process produces an observable electronic signal, with energy in the eV–keV range, in addition to the tiny nuclear recoil. Later works has revealed its importance for the dark matter direct detection [35–73]. Leveraging the Migdal effect, several searches for sub-GeV dark matter have been performed [74–81]. However, Migdal effect itself remained experimentally unverified in neutron-nucleus scattering until recently, when it was observed in a gaseous detector [82]. This breakthrough has spurred further validation in liquid xenon experiments [83] and other detectors [84, 85].

While direct detection experiments have made significant progress in searching for light dark matter in the galactic halo, nuclear reactors provide a complementary and unique source characterized by an intense high flux of light new particles [86–91]. Unlike the non-relativistic halo dark matter, the dark matter particles produced in nuclear reactors, arising via the decay of light mediators emitted during nuclear de-excitation, $N^* \to N + V(\to \chi\bar{\chi})$, can possess MeV-scale energies since the mediator energy is fixed by the discrete nuclear transition energy, $E_V \simeq \omega_i$. This high-flux, relativistic component offers a distinct opportunity to probe the sub-MeV parameter space that is inaccessible to standard halo searches. However, detecting these reactor-produced particles via standard elastic scattering in semiconductor detectors is hindered by the quenching effect. Since a substantial fraction of the nuclear-recoil energy is dissipated into lattice vibrations, the deposited ionization energy in electron equivalent is typically only a few hundred $\mathrm{eV_{ee}}$. This lies below the threshold of conventional experiments, such as TEXONO germanium detector [92].

In this work, we study Migdal ionization as an observable channel for reactor-produced sub-MeV dark matter in low-threshold germanium detectors. The sudden acceleration of the nucleus can tear off bound electrons, generating an accompanying ionization signal that raises the deposited energy above threshold. The incoming dark matter flux is computed from neutron-capture nuclear de-excitation in ^{238}U and ^{10}B. Using the TEXONO reactor ON-OFF residual spectrum [92], we derive 95% C.L. limits on the reference dark matter-proton cross section $\bar{\sigma}_{\chi p}$ for dark matter masses $0.01\,\mathrm{MeV} < m_\chi < 2.6\,\mathrm{MeV}$. Importantly, since the incident χ flux is generated in the reactor, the limits derived here are independent of the cosmological abundance of χ and do not require χ to constitute all the observed dark matter density. This paper is organized as follows. Section 2 describes reactor nuclear de-excitation and the resulting dark matter flux. Section 3 presents the Migdal signal and the resulting TEXONO limits. We conclude in section 4.

2 Dark matter production

We consider a kinetically mixed dark photon V [9] coupled to a Dirac fermion dark matter state χ. The relevant Lagrangian is

$$\mathcal{L} \supset -\frac{1}{4}V_{\mu\nu}V^{\mu\nu} + \frac{1}{2}m_V^2 V_\mu V^\mu - \frac{\epsilon}{2}V_{\mu\nu}F^{\mu\nu} + g_\chi V_\mu \bar{\chi}\gamma^\mu \chi, \tag{2.1}$$

where $g_\chi = \sqrt{4\pi\alpha_D}$, m_V is the dark photon mass, which can be generated via the Stueckelberg or dark Higgs mechanism [93–95], and ϵ is the kinetic mixing parameter. After diagonalizing the gauge kinetic terms, V couples to the electromagnetic current with strength ϵe. We focus on the invisible decay regime $m_V > 2m_\chi$ and take $\alpha_D \gg \epsilon^2\alpha$, so that $\mathrm{BR}(V \to \chi\bar{\chi}) \simeq 1$. For the parameter space considered here, the mediator decays promptly near the reactor source.

In the vector-portal scenario, neutron-capture de-excitation provides a line source of vector mediators: an excited nuclear state N^* can de-excite by emitting either a photon or, through kinetic mixing, an on-shell vector mediator V, via $n + N \to N^* \to N + V$, followed by $V \to \chi\bar{\chi}$. The emitted mediator carries energy $E_{V,i} \simeq \omega_i$, where ω_i is the i-th nuclear transition energy, with nuclear recoil corrections negligible at MeV scales. On-shell production is kinematically allowed whenever $m_V < \omega_i$.

For the i-th transition, the mediator production rate at the reactor is

$$\dot{N}_{V,i} = \dot{N}_{\gamma,i}\, r_{E1,i}, \tag{2.2}$$

where $\dot{N}_{\gamma,i}$ is the ordinary photon emission rate and $r_{E1,i}$ is the dark-vector-to-photon emission ratio. For an E1 transition of energy ω_i [86, 87, 96],

$$r_{E1,i} = \epsilon^2 \left(1 + \frac{m_V^2}{2\omega_i^2}\right)\sqrt{1 - \frac{m_V^2}{\omega_i^2}}\,\Theta(\omega_i - m_V). \tag{2.3}$$

The ordinary photon emission rate is

$$\dot{N}_{\gamma,i} = N_n \frac{Y_n^{(N)}}{\sum_N Y_n^{(N)}} \frac{I_\gamma^{(N,\omega_i)}}{100}. \tag{2.4}$$

JHEP11(2026)014

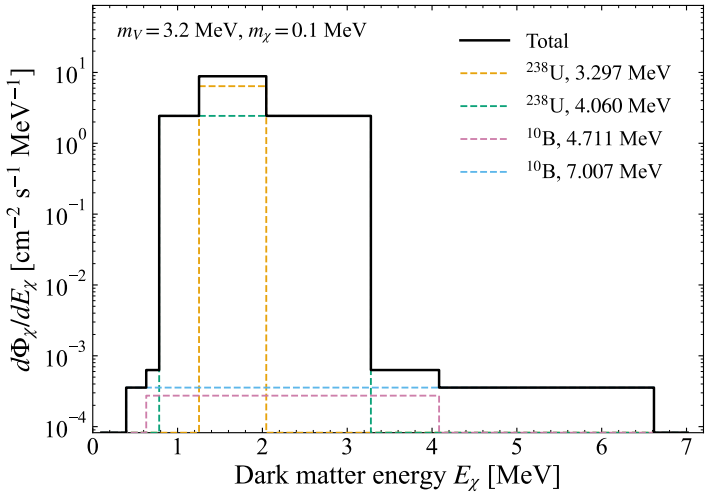


Figure 1. Reactor dark matter flux from neutron-capture nuclear de-excitation for the benchmark parameters $(m_V, m_\chi) = (3.2, 0.1)$ MeV, $\epsilon = 10^{-5}$, and $\alpha_D = 0.1$. Each transition produces a box-shaped spectrum from $V \to \chi\bar{\chi}$, and the total flux is the sum over the retained lines.

Here $N_n = 7.8 \times 10^{19}\, P(\mathrm{GW})\ \mathrm{s}^{-1}$ is the total neutron production rate, corresponding to an average fission energy of 200 MeV and 2.5 neutrons per fission [97, 98]. For the TEXONO benchmark with $P = 2.9$ GW, $N_n \simeq 2.3 \times 10^{20}\ \mathrm{s}^{-1}$. $Y_n^{(N)}$ is the neutron-capture yield per fission for isotope N, and $I_\gamma^{(N,\omega_i)}$ is the number of photons of energy ω_i emitted per 100 radiative neutron captures on that isotope [98–100]. For ^{10}B, this photon yield includes the small radiative-capture contribution to $^{10}\mathrm{B}(n,\gamma)^{11}\mathrm{B}$, while the dominant $^{10}\mathrm{B}(n,\alpha)^{7}\mathrm{Li}$ channel does not contribute to the MeV-scale gamma lines here [100].

The two-body decay $V \to \chi\bar{\chi}$ produces a box-shaped dark matter spectrum with endpoints

$$E_{\chi,i}^{\mathrm{min,max}} = \frac{E_{V,i}}{2} \mp \frac{\sqrt{E_{V,i}^2 - m_V^2}\sqrt{m_V^2 - 4m_\chi^2}}{2m_V}, \tag{2.5}$$

and width $\Delta E_{\chi,i} = E_{\chi,i}^{\max} - E_{\chi,i}^{\min}$. The differential dark matter flux at the detector from the i-th transition is

$$\frac{d\Phi_{\chi,i}}{dE_\chi} = \frac{2\,\dot{N}_{V,i}\,\mathrm{BR}(V \to \chi\bar{\chi})}{4\pi L^2\,\Delta E_{\chi,i}}, \quad E_{\chi,i}^{\min} \le E_\chi \le E_{\chi,i}^{\max}, \tag{2.6}$$

where $L = 28$ m is the baseline between the Kuo-Sheng reactor core and the TEXONO germanium detector [92],the factor of two accounts for both χ and $\bar{\chi}$, and the total flux is $d\Phi_\chi/dE_\chi = \sum_i d\Phi_{\chi,i}/dE_\chi$.

We use a benchmark set of intense E1 neutron-capture transitions: the 3.297 and 4.060 MeV lines from $^{238}\mathrm{U}(n,\gamma)^{239}\mathrm{U}$, and the 4.711 and 7.007 MeV lines from $^{10}\mathrm{B}(n,\gamma)^{11}\mathrm{B}$. The present source model includes only mediators produced directly in these primary nuclear de-excitation transitions. Secondary production via $\gamma e^- \to V e^-$, as well as contributions from additional capture isotopes or other multipolarities, are not included. A more complete nuclear de-excitation database could modify both the normalization and the spectral shape of the predicted flux. The resulting benchmark dark matter flux is shown in figure 1.

JHEP11(2026)014

3 Migdal signal and TEXONO limits

We compute the response of a low-threshold germanium detector to the reactor-produced dark matter flux derived in section 2. The response is built from elastic nuclear scattering, nuclear recoil quenching, and the single-ionization Migdal contribution. For a single-ionization Migdal process, the total deposited energy is

$$E_{\rm det} = q_{\rm nr}(E_{\rm nr})E_{\rm nr} + E_{nl} + E_e, \tag{3.1}$$

where $E_{\rm nr}$ is the nuclear recoil energy, E_{nl} is the binding energy of the shell (n, l), and E_e is the kinetic energy of the emitted electron. Since the detector is sensitive to ionization, only the fraction of the nuclear-recoil energy transferred to electronic excitations contributes to the measured signal. This effect is characterized by the nuclear-recoil quenching factor $q_{\rm nr}(E_{\rm nr})$, which gives the fraction of the recoil energy that is visible in the detector. We evaluate $q_{\rm nr}$ using the Lindhard prescription [101],

$$q_{\rm nr}(E_{\rm nr}) = \frac{k\, g(\varepsilon)}{1 + k\, g(\varepsilon)}, \qquad g(\varepsilon) = 3\varepsilon^{0.15} + 0.7\varepsilon^{0.6} + \varepsilon, \tag{3.2}$$

with $\varepsilon = 11.5\, Z^{-7/3}(E_{\rm nr}/\text{keV})$ and $k = 0.133\, Z^{2/3}A^{-1/2}$, which gives $k \simeq 0.157$ for germanium.

The corresponding differential Migdal event rate is then obtained by combining the reactor dark matter flux, the nuclear scattering cross section, and the Migdal ionization probability,

$$\begin{aligned}\frac{dR_{\rm Migdal}}{dE_{\rm det}} = N_T \int dE_\chi \frac{d\Phi_\chi}{dE_\chi} \int dE_{\rm nr} \frac{d\sigma_{\chi A}}{dE_{\rm nr}} \\ \times \sum_{n,l} \int dE_e \frac{dp_v(nl \to E_e)}{dE_e} \delta(E_{\rm det} - q_{\rm nr}(E_{\rm nr})E_{\rm nr} - E_{nl} - E_e)\,.\end{aligned} \tag{3.3}$$

Here N_T is the number of germanium target nuclei per unit detector mass, p_v denotes the Migdal ionization probability, and $dp_v(nl \to E_e)/dE_e$ is the differential probability for ionizing an electron from the (n, l) shell with kinetic energy E_e. We compute the Migdal single-ionization probabilities in the isolated-atom approximation. For each occupied germanium orbital from the K through N shells ($1s$, $2s$, $2p$, $3s$, $3p$, $3d$, $4s$, and $4p$), the bound and continuum electron wave functions are generated with cFAC version 1.7.1 [102], a C-based fork of the Flexible Atomic Code [103], and the ionization probability is evaluated from the overlap between the boosted initial electronic state and the final continuum state induced by the sudden nuclear recoil.

Previous studies of the Migdal effect in noble-element targets such as xenon and argon have commonly described the electronic response using atomic ionization probabilities [39, 104], while subsequent studies of semiconductor targets have explicitly included the crystal environment [42, 47]. Here we use isolated-atom Migdal ionization probabilities for germanium and assess this approximation by comparing the relevant atomic and crystal scales. The germanium lattice constant $a \simeq 0.566$ nm corresponds to $p_{\rm lat} \sim \hbar(2\pi/a) \simeq 2.2$ keV$/c$, whereas the M-shell binding energies $E_B \simeq 35$–170 eV imply $p_{\rm atom} \sim \sqrt{2m_e E_B} \simeq 6$–$13$ keV$/c$. With the germanium band gap $E_g \simeq 0.67$ eV [105], these binding energies are also about 50–250 times larger than E_g. These scale comparisons support the isolated-atom treatment for the inner-shell contribution considered here. To remain conservative, we impose $v_N/c \geq 10^{-4}$.

JHEP11(2026)014

The nuclear scattering cross section entering eq. (3.3) is normalized by the reference DM-proton cross section

$$\bar{\sigma}_{\chi p} = \frac{16\pi\alpha\alpha_D\epsilon^2\mu_{\chi p}^2}{(q_0^2 + m_V^2)^2}, \qquad q_0 = \alpha m_e. \tag{3.4}$$

For a germanium target with $Z = 32$ and nuclear mass m_A, we use

$$\frac{d\sigma_{\chi A}}{dE_{\rm nr}} = \frac{Z^2\bar{\sigma}_{\chi p}F^2(E_{\rm nr})|F_{\rm DM}(q)|^2}{4\mu_{\chi A}^2(E_\chi^2 - m_\chi^2)}\mathcal{K}(E_{\rm nr}), \tag{3.5}$$

with the Helm form factor $F(E_{\rm nr})$ [106], $q = \sqrt{2m_A E_{\rm nr}}$, the mediator form factor $|F_{\rm DM}(q)|^2 = (q_0^2 + m_V^2)^2/(q^2 + m_V^2)^2$, and the kinematic factor $\mathcal{K}(E_{\rm nr}) = 2m_A E_\chi^2 - E_{\rm nr}(2m_A E_\chi + m_\chi^2 + m_A^2 - m_A E_{\rm nr})$. The Migdal probability is multiplied as an atomic transition factor and does not introduce an additional nuclear form factor.

For the benchmark $(m_V, m_\chi) = (3.2, 0.1)\,\text{MeV}$, the highest retained de-excitation line, 7.007 MeV, gives $E_\chi^{\rm max} \simeq 6.61$ MeV and hence $E_{\rm nr}^{\rm max} \simeq 1.29\ \text{keV}_{\rm nr}$. After Lindhard quenching, the maximum detected energy from the elastic nuclear recoil is about $0.23\ \text{keV}_{\rm ee}$, below the TEXONO threshold. Thus, the elastic NR curve in figure 2 ends at the quenched-recoil kinematic endpoint. Migdal ionization adds the electronic energy $(E_{nl} + E_e)$ to the detected signal, allowing events to enter the observable window. For this benchmark, the above-threshold Migdal rate is dominated by the M and L shells, contributing about 85.6% and 13.0%, respectively, while the N and K shells contribute only 1.15% and 0.23%. The M-shell binding energies lie in the range $\sim$ 35–170 eV, and the prominent change of slope near $E_{\rm det} \simeq 1.2$–1.4 keV is associated with the L-shell contribution, dominated by the $2p$ orbital. The K-shell threshold near 11 keV lies in the low-rate tail.

To constrain this channel, we derive constraints from the publicly available TEXONO reactor ON-OFF residual spectrum, defined as the difference between the spectra measured with the reactor operating and shut down, using data from the low-threshold germanium detector at the Kuo-Sheng Reactor Neutrino Laboratory [92]. Since the dark matter flux is produced by the reactor, it is retained in this residual, while reactor-independent backgrounds are reduced by the subtraction. We therefore use the residual spectrum as the observable for the constraint analysis. For each mass point (m_χ, m_V), the bin-averaged signal is

$$S_b(\epsilon, m_V, m_\chi) = \frac{1}{\Delta E_b}\int_{E_b^{\rm min}}^{E_b^{\rm max}} dE_{\rm det}\,\frac{dR_{\rm Migdal}}{dE_{\rm det}}, \tag{3.6}$$

where $E_b^{\rm min}$ and $E_b^{\rm max}$ are the lower and upper edges of the b-th detector-energy bin and $\Delta E_b = E_b^{\rm max} - E_b^{\rm min}$. We define the Gaussian chi-square as

$$\chi^2(\epsilon, m_V, m_\chi) = \sum_b \frac{[R_b - S_b(\epsilon, m_V, m_\chi)]^2}{\sigma_b^2}, \tag{3.7}$$

where R_b and σ_b are the measured ON-OFF residual rate and its uncertainty in the b-th bin. We minimize χ^2 over $\epsilon \geq 0$ and obtain the one-sided 95% C.L. upper limit $\epsilon_{\rm lim}$ from $\Delta\chi^2(\epsilon_{\rm lim}) = 2.71$, with $\Delta\chi^2(\epsilon) = \chi^2(\epsilon) - \chi^2_{\rm min}$. The mediator mass scan covers $3.2\ \text{MeV} \leq m_V \leq 6.9\ \text{MeV}$, with the lower bound chosen to isolate the neutron-capture

JHEP11(2026)014

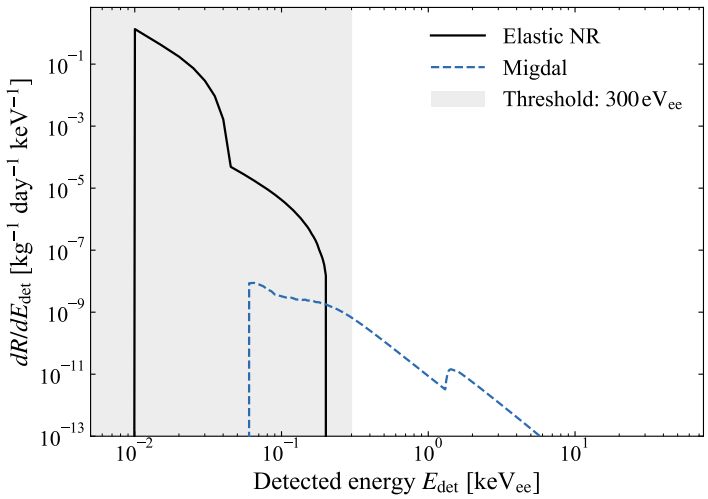


Figure 2. Differential event rate of reactor-produced light dark matter in the TEXONO germanium detector. The quenched elastic nuclear-recoil contribution lies below the 300 $\mathrm{eV_{ee}}$ analysis threshold for the benchmark shown, while Migdal ionization populates the observable electron-equivalent energy region. The resulting shell-resolved tables for $dP_v(nl \to E_e)/dE_e$ are used in eq. (3.3), retaining only kinematically allowed single-ionization events; the successive onset of each orbital's threshold, $E_{\rm det} \gtrsim E_{nl} + q_{\rm nr}E_{\rm nr}$, produces the characteristic changes of slope in the Migdal spectrum shown in figure 2. Since the quenched elastic recoil lies below threshold for the reactor-produced MeV-scale flux, the observable signal is dominated by Migdal ionization.

de-excitation source from the lower-mass region where Compton-like reactor production can also contribute [86], and the upper bound set below $\omega_{\rm max} = 7.007$ MeV, where the available de-excitation phase space vanishes.

The resulting 95% C.L. upper limits on $\bar{\sigma}_{\chi p}$ are shown in figure 3. For fixed m_χ, larger m_V values are supported mainly by the higher-energy retained transitions, which typically yield more energetic $\chi\bar{\chi}$ pairs. This enhances the Migdal signal in the observable energy window and strengthens the limits over most of the scan range. Close to the endpoint of the highest retained transition, however, the production phase space is suppressed, and the limits weaken as m_V approaches $\omega_{\rm max}$. Theoretically, the mass of dark matter can reach $m_\chi < \omega_{\rm max}/2 \simeq 3.50$ MeV. However, the present analysis loses sensitivity for $m_\chi \gtrsim 2.56$ MeV because of the negligible event rate. As m_χ approaches this upper end of the scan, the available phase space and the above-threshold event rate decrease rapidly, producing the upward slope of the limit curves.

For comparison, we show the CMB+BAO and Lyman-α constraints of ref. [107], together with the SENSEI direct detection limit [108]. These existing bounds are not derived within the same theoretical framework as our reactor constraint. The CMB+BAO and Lyman-α bounds are obtained for a velocity-independent DM-proton interaction ($n = 0$), with the assumed interacting dark matter fraction f_χ indicated in figure 3. The SENSEI limit assumes Galactic halo dark matter scattering from silicon nuclei through a heavy scalar mediator, with the observable ionization signal generated by the Migdal effect. By contrast, our reactor limits are obtained in the kinetically mixed dark photon scenario and depend on the laboratory-produced $\chi\bar{\chi}$ flux rather than on the Galactic halo or cosmological abundance of

JHEP11(2026)014

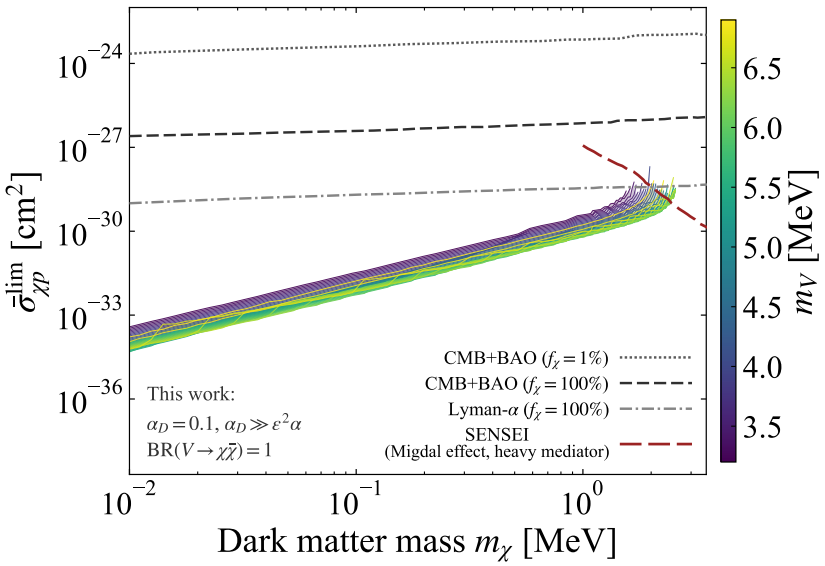


Figure 3. TEXONO 95% C.L. upper limits on $\bar{\sigma}^{\rm lim}_{\chi p}$ from reactor-produced light dark matter via Migdal ionization in the low-threshold germanium detector, shown as a function of m_χ for m_V in the range 3.2–6.9 MeV (color scale). The limits are obtained in the kinetically mixed dark photon scenario with $\alpha_D = 0.1$ and $\alpha_D \gg \epsilon^2\alpha$, taking the invisible branching ratio to be BR$(V \to \chi\bar{\chi}) = 1$. Existing constraints are shown for comparison but are not derived within the same theoretical framework. The CMB+BAO and Lyman-α 95% C.L. bounds constrain a velocity-independent DM-proton interaction ($n = 0$) [107], with the assumed interacting dark matter fraction f_χ indicated in the figure. The SENSEI 90% C.L. Migdal (MG) limit assumes Galactic halo dark matter scattering from silicon nuclei through a heavy scalar mediator, with the observable ionization signal generated by the Migdal effect [108]. In contrast to the cosmological bounds, the reactor limits depend on the laboratory-produced $\chi\bar{\chi}$ flux and do not require χ to constitute any specified fraction of the cosmological dark matter abundance.

χ. Relevant cosmological constraints also include BBN and $N_{\rm eff}$ bounds, which depend on the thermalization, decoupling, and entropy-transfer history of the dark sector [109, 110], while freeze-in targets depend on both the production history and the relic abundance assigned to χ [111]. Astrophysical constraints from stellar and supernova cooling depend on the in-medium production, absorption, trapping, and transport of dark-sector states [111, 112]. In particular, when dark self-interactions are strong, the produced states may form a coupled dark fluid rather than free-streaming particles, which can substantially modify the resulting constraints [113].

4 Conclusion

We have studied Migdal ionization as an observable channel for reactor-produced sub-MeV dark matter in low-threshold germanium detectors. The reactor source is provided by neutron-capture nuclear de-excitation, in which excited nuclei can emit on-shell kinetically mixed vector mediators in place of ordinary photons. The mediators subsequently decay invisibly into $\chi\bar{\chi}$, producing dark matter with box-shaped energy spectra.

JHEP11(2026)014

Using selected E1 transitions from $^{238}\mathrm{U}(n,\gamma)^{239}\mathrm{U}$ and $^{10}\mathrm{B}(n,\gamma)^{11}\mathrm{B}$, we computed the resulting reactor dark matter flux at the TEXONO baseline, and calculated the germanium detector response including elastic nuclear scattering, nuclear recoil quenching, and Migdal ionization. For the benchmark spectra considered here, the nuclear recoil contribution alone remains below the 300 $\mathrm{eV_{ee}}$ analysis threshold, while Migdal ionization adds electronic energy to the detector response and provides the relevant visible channel. From the TEXONO reactor ON-OFF residual spectrum, we derived 95% C.L. upper limits on the reference DM-proton cross section $\bar{\sigma}_{\chi p}$, ranging roughly from 6.7×10^{-35} to 8.0×10^{-33} cm^2, for MeV-scale mediators and dark matter masses 0.01 MeV $< m_\chi <$ 2.6 MeV. These limits rely only on the reactor-produced $\chi\bar{\chi}$ flux and the germanium detector response, and do not assume that χ constitutes the cosmological dark matter abundance.

Acknowledgments

This work is supported by the NNSFC under Grant No. 12275134 and No. 12335005.

Data Availability Statement. This article has no associated data or the data will not be deposited.

Code Availability Statement. This article has no associated code or the code will not be deposited.

Open Access. This article is distributed under the terms of the Creative Commons Attribution License (CC-BY4.0), which permits any use, distribution and reproduction in any medium, provided the original author(s) and source are credited.

References

[1] G. Bertone, D. Hooper and J. Silk, *Particle dark matter: Evidence, candidates and constraints*, *Phys. Rept.* **405** (2005) 279 [hep-ph/0404175] [INSPIRE].

[2] M. Battaglieri et al., *US Cosmic Visions: New Ideas in Dark Matter 2017: Community Report*, in the proceedings of the *U.S. Cosmic Visions: New Ideas in Dark Matter*, College Park, U.S.A., 23–25 March 2017 [arXiv:1707.04591] [INSPIRE].

[3] LUX collaboration, *Results from a search for dark matter in the complete LUX exposure*, *Phys. Rev. Lett.* **118** (2017) 021303 [arXiv:1608.07648] [INSPIRE].

[4] XENON collaboration, *Dark Matter Search Results from a One Ton-Year Exposure of XENON1T*, *Phys. Rev. Lett.* **121** (2018) 111302 [arXiv:1805.12562] [INSPIRE].

[5] PandaX-4T collaboration, *Dark Matter Search Results from the PandaX-4T Commissioning Run*, *Phys. Rev. Lett.* **127** (2021) 261802 [arXiv:2107.13438] [INSPIRE].

[6] C. Boehm and P. Fayet, *Scalar dark matter candidates*, *Nucl. Phys. B* **683** (2004) 219 [hep-ph/0305261] [INSPIRE].

[7] M. Pospelov, A. Ritz and M.B. Voloshin, *Secluded WIMP Dark Matter*, *Phys. Lett. B* **662** (2008) 53 [arXiv:0711.4866] [INSPIRE].

[8] N. Arkani-Hamed, D.P. Finkbeiner, T.R. Slatyer and N. Weiner, *A Theory of Dark Matter*, *Phys. Rev. D* **79** (2009) 015014 [arXiv:0810.0713] [INSPIRE].

JHEP11(2026)014

[9] B. Holdom, *Two U(1)'s and Epsilon Charge Shifts*, *Phys. Lett. B* **166** (1986) 196 [INSPIRE].

[10] J. Alexander et al., *Dark Sectors 2016 Workshop: Community Report*, arXiv:1608.08632 [INSPIRE].

[11] Y. Hochberg, E. Kuflik, T. Volansky and J.G. Wacker, *Mechanism for Thermal Relic Dark Matter of Strongly Interacting Massive Particles*, *Phys. Rev. Lett.* **113** (2014) 171301 [arXiv:1402.5143] [INSPIRE].

[12] Y. Hochberg et al., *Model for Thermal Relic Dark Matter of Strongly Interacting Massive Particles*, *Phys. Rev. Lett.* **115** (2015) 021301 [arXiv:1411.3727] [INSPIRE].

[13] E. Kuflik, M. Perelstein, N.R.-L. Lorier and Y.-D. Tsai, *Elastically Decoupling Dark Matter*, *Phys. Rev. Lett.* **116** (2016) 221302 [arXiv:1512.04545] [INSPIRE].

[14] E. Kuflik, M. Perelstein, N.R.-L. Lorier and Y.-D. Tsai, *Phenomenology of ELDER Dark Matter*, *JHEP* **08** (2017) 078 [arXiv:1706.05381] [INSPIRE].

[15] K. Griest and D. Seckel, *Three exceptions in the calculation of relic abundances*, *Phys. Rev. D* **43** (1991) 3191 [INSPIRE].

[16] R.T. D'Agnolo and J.T. Ruderman, *Light Dark Matter from Forbidden Channels*, *Phys. Rev. Lett.* **115** (2015) 061301 [arXiv:1505.07107] [INSPIRE].

[17] J.A. Dror, E. Kuflik and W.H. Ng, *Codecaying Dark Matter*, *Phys. Rev. Lett.* **117** (2016) 211801 [arXiv:1607.03110] [INSPIRE].

[18] R.T. D'Agnolo, D. Pappadopulo and J.T. Ruderman, *Fourth Exception in the Calculation of Relic Abundances*, *Phys. Rev. Lett.* **119** (2017) 061102 [arXiv:1705.08450] [INSPIRE].

[19] R. Essig et al., *First Direct Detection Limits on sub-GeV Dark Matter from XENON10*, *Phys. Rev. Lett.* **109** (2012) 021301 [arXiv:1206.2644] [INSPIRE].

[20] R. Essig et al., *Direct Detection of sub-GeV Dark Matter with Semiconductor Targets*, *JHEP* **05** (2016) 046 [arXiv:1509.01598] [INSPIRE].

[21] H. An, M. Pospelov, J. Pradler and A. Ritz, *Directly Detecting MeV-scale Dark Matter via Solar Reflection*, *Phys. Rev. Lett.* **120** (2018) 141801 [*Erratum ibid.* **121** (2018) 259903] [arXiv:1708.03642] [INSPIRE].

[22] S. Knapen, T. Lin and K.M. Zurek, *Light Dark Matter: Models and Constraints*, *Phys. Rev. D* **96** (2017) 115021 [arXiv:1709.07882] [INSPIRE].

[23] T. Bringmann and M. Pospelov, *Novel direct detection constraints on light dark matter*, *Phys. Rev. Lett.* **122** (2019) 171801 [arXiv:1810.10543] [INSPIRE].

[24] C.V. Cappiello and J.F. Beacom, *Strong New Limits on Light Dark Matter from Neutrino Experiments*, *Phys. Rev. D* **100** (2019) 103011 [*Erratum ibid.* **104** (2021) 069901] [arXiv:1906.11283] [INSPIRE].

[25] J. Alvey, M. Campos, M. Fairbairn and T. You, *Detecting Light Dark Matter via Inelastic Cosmic Ray Collisions*, *Phys. Rev. Lett.* **123** (2019) 261802 [arXiv:1905.05776] [INSPIRE].

[26] L. Su et al., *Atmospheric Dark Matter and Xenon1T Excess*, *Phys. Rev. D* **102** (2020) 115028 [arXiv:2006.11837] [INSPIRE].

[27] S.-F. Ge, J. Liu, Q. Yuan and N. Zhou, *Diurnal Effect of Sub-GeV Dark Matter Boosted by Cosmic Rays*, *Phys. Rev. Lett.* **126** (2021) 091804 [arXiv:2005.09480] [INSPIRE].

[28] Y. Kahn and T. Lin, *Searches for light dark matter using condensed matter systems*, *Rept. Prog. Phys.* **85** (2022) 066901 [arXiv:2108.03239] [INSPIRE].

JHEP11(2026)014

[29] W. Wang, L. Wu, W.-N. Yang and B. Zhu, *Spin-dependent scattering of boosted dark matter*, *Phys. Rev. D* **107** (2023) 073002 [arXiv:2111.04000] [INSPIRE].

[30] L. Su, L. Wu and B. Zhu, *An improved bound on accelerated light dark matter*, *Sci. China Phys. Mech. Astron.* **67** (2024) 221012 [arXiv:2308.02204] [INSPIRE].

[31] K.I. Nagao, T. Naka and T. Nomura, *Directional direct detection of MeV scale boosted dark matter in two component dark matter scenario via dark photon interaction*, *JCAP* **04** (2025) 030 [arXiv:2411.10149] [INSPIRE].

[32] Z.-L. Liang, L. Su, L. Wu and B. Zhu, *Plasmon-enhanced Direct Detection of sub-MeV Dark Matter*, *Phys. Rev. Lett.* **134** (2025) 071001 [arXiv:2401.11971] [INSPIRE].

[33] A. Migdal, *Ionizatsiya atomov pri yadernykh reaktsiyakh*, *Sov. Phys. JETP* **9** (1939) 1163.

[34] A.B. Migdal, *Ionization of atoms accompanying alpha and beta decay*, *J. Phys. USSR* **4** (1941) 449.

[35] J.D. Vergados and H. Ejiri, *The role of ionization electrons in direct neutralino detection*, *Phys. Lett. B* **606** (2005) 313 [hep-ph/0401151] [INSPIRE].

[36] C.C. Moustakidis, J.D. Vergados and H. Ejiri, *Direct dark matter detection by observing electrons produced in neutralino-nucleus collisions*, *Nucl. Phys. B* **727** (2005) 406 [hep-ph/0507123] [INSPIRE].

[37] H. Ejiri, C.C. Moustakidis and J.D. Vergados, *Dark matter search by exclusive studies of X-rays following WIMPs nuclear interactions*, *Phys. Lett. B* **639** (2006) 218 [hep-ph/0510042] [INSPIRE].

[38] R. Bernabei et al., *On electromagnetic contributions in WIMP quests*, *Int. J. Mod. Phys. A* **22** (2007) 3155 [arXiv:0706.1421] [INSPIRE].

[39] M. Ibe, W. Nakano, Y. Shoji and K. Suzuki, *Migdal Effect in Dark Matter Direct Detection Experiments*, *JHEP* **03** (2018) 194 [arXiv:1707.07258] [INSPIRE].

[40] M.J. Dolan, F. Kahlhoefer and C. McCabe, *Directly detecting sub-GeV dark matter with electrons from nuclear scattering*, *Phys. Rev. Lett.* **121** (2018) 101801 [arXiv:1711.09906] [INSPIRE].

[41] N.F. Bell et al., *Migdal effect and photon bremsstrahlung in effective field theories of dark matter direct detection and coherent elastic neutrino-nucleus scattering*, *Phys. Rev. D* **101** (2020) 015012 [arXiv:1905.00046] [INSPIRE].

[42] R. Essig, J. Pradler, M. Sholapurkar and T.-T. Yu, *Relation between the Migdal Effect and Dark Matter-Electron Scattering in Isolated Atoms and Semiconductors*, *Phys. Rev. Lett.* **124** (2020) 021801 [arXiv:1908.10881] [INSPIRE].

[43] D. Baxter, Y. Kahn and G. Krnjaic, *Electron Ionization via Dark Matter-Electron Scattering and the Migdal Effect*, *Phys. Rev. D* **101** (2020) 076014 [arXiv:1908.00012] [INSPIRE].

[44] Z.-L. Liang, L. Zhang, F. Zheng and P. Zhang, *Describing Migdal effects in diamond crystal with atom-centered localized Wannier functions*, *Phys. Rev. D* **102** (2020) 043007 [arXiv:1912.13484] [INSPIRE].

[45] V.V. Flambaum, L. Su, L. Wu and B. Zhu, *New strong bounds on sub-GeV dark matter from boosted and Migdal effects*, *Sci. China Phys. Mech. Astron.* **66** (2023) 271011 [arXiv:2012.09751] [INSPIRE].

[46] C.P. Liu, C.-P. Wu, H.-C. Chi and J.-W. Chen, *Model-independent determination of the Migdal effect via photoabsorption*, *Phys. Rev. D* **102** (2020) 121303 [arXiv:2007.10965] [INSPIRE].

JHEP11(2026)014

[47] S. Knapen, J. Kozaczuk and T. Lin, *Migdal Effect in Semiconductors*, *Phys. Rev. Lett.* **127** (2021) 081805 [arXiv:2011.09496] [INSPIRE].

[48] Z.-L. Liang, C. Mo, F. Zheng and P. Zhang, *Describing the Migdal effect with a bremsstrahlung-like process and many-body effects*, *Phys. Rev. D* **104** (2021) 056009 [arXiv:2011.13352] [INSPIRE].

[49] J. Liao, H. Liu and D. Marfatia, *Coherent neutrino scattering and the Migdal effect on the quenching factor*, *Phys. Rev. D* **104** (2021) 015005 [arXiv:2104.01811] [INSPIRE].

[50] J.F. Acevedo, J. Bramante and A. Goodman, *Accelerating composite dark matter discovery with nuclear recoils and the Migdal effect*, *Phys. Rev. D* **105** (2022) 023012 [arXiv:2108.10889] [INSPIRE].

[51] W. Wang, K.-Y. Wu, L. Wu and B. Zhu, *Direct detection of spin-dependent sub-GeV dark matter via Migdal effect*, *Nucl. Phys. B* **983** (2022) 115907 [arXiv:2112.06492] [INSPIRE].

[52] J. Li, L. Su, L. Wu and B. Zhu, *Spin-dependent sub-GeV inelastic dark matter-electron scattering and Migdal effect. Part I. Velocity independent operator*, *JCAP* **04** (2023) 020 [arXiv:2210.15474] [INSPIRE].

[53] P. Cox, M.J. Dolan, C. McCabe and H.M. Quiney, *Precise predictions and new insights for atomic ionization from the Migdal effect*, *Phys. Rev. D* **107** (2023) 035032 [arXiv:2208.12222] [INSPIRE].

[54] Z.-L. Liang, C. Mo, F. Zheng and P. Zhang, *Phonon-mediated Migdal effect in semiconductor detectors*, *Phys. Rev. D* **106** (2022) 043004 [*Erratum ibid.* **106** (2022) 109901] [arXiv:2205.03395] [INSPIRE].

[55] C. Blanco et al., *Molecular Migdal effect*, *Phys. Rev. D* **106** (2022) 115015 [arXiv:2208.09002] [INSPIRE].

[56] G. Tomar, S. Kang and S. Scopel, *Low-mass extension of direct detection bounds on WIMP-quark and WIMP-gluon effective interactions using the Migdal effect*, *Astropart. Phys.* **150** (2023) 102851 [arXiv:2210.00199] [INSPIRE].

[57] D. Adams et al., *Measuring the Migdal effect in semiconductors for dark matter detection*, *Phys. Rev. D* **107** (2023) L041303 [arXiv:2210.04917] [INSPIRE].

[58] K.V. Berghaus, A. Esposito, R. Essig and M. Sholapurkar, *The Migdal effect in semiconductors for dark matter with masses below $\sim$ 100 MeV*, *JHEP* **01** (2023) 023 [arXiv:2210.06490] [INSPIRE].

[59] Y. Gu, J. Tang, L. Wu and B. Zhu, *Probing light DM via the Migdal effect with spherical proportional counter*, *Chin. Phys. C* **47** (2023) 125105 [arXiv:2309.09740] [INSPIRE].

[60] J. Xu et al., *Search for the Migdal effect in liquid xenon with keV-level nuclear recoils*, *Phys. Rev. D* **109** (2024) L051101 [arXiv:2307.12952] [INSPIRE].

[61] M. Qiao, C. Xia and Y.-F. Zhou, *Diurnal modulation of electron recoils from DM-nucleon scattering through the Migdal effect*, *JCAP* **11** (2023) 079 [arXiv:2307.12820] [INSPIRE].

[62] Y.-F. Li and S.-Y. Xia, *Migdal effect of phonon-mediated neutrino nucleus scattering in semiconductor detectors*, *Nucl. Phys. B* **1006** (2024) 116632 [arXiv:2310.05704] [INSPIRE].

[63] G. Herrera, *A neutrino floor for the Migdal effect*, *JHEP* **05** (2024) 288 [arXiv:2311.17719] [INSPIRE].

[64] V.A. Dzuba, V.V. Flambaum and I.B. Samsonov, *Migdal-type effect in the dark matter absorption process*, *Phys. Rev. D* **109** (2024) 115032 [arXiv:2312.10566] [INSPIRE].

JHEP11(2026)014

[65] Y. Kahn and J. Pérez-Ríos, *Measuring the molecular Migdal effect with neutron scattering on diatomic gases*, *Phys. Rev. D* **110** (2024) 092012 [arXiv:2403.08866] [INSPIRE].

[66] S. Kang, S. Scopel and G. Tomar, *Low-mass constraints on WIMP effective models of inelastic scattering using the Migdal effect*, *JCAP* **01** (2025) 035 [arXiv:2407.16187] [INSPIRE].

[67] W. Nakano, *Comparison of the Migdal transition probabilities in electron-atom inelastic cross sections*, *JHEP* **10** (2025) 130 [arXiv:2410.16911] [INSPIRE].

[68] T.N. Maity, *Neutrinos as background and signal in searches using the Migdal effect*, *Phys. Rev. D* **111** (2025) 123020 [arXiv:2412.17649] [INSPIRE].

[69] A. Esposito and A. Rocchi, *Migdal effect in solid crystals and the role of nonadiabaticity*, *Phys. Rev. D* **112** (2025) 075034 [arXiv:2505.08864] [INSPIRE].

[70] Q.I.A.O. Mai, G.U.O. Huai-Ke and Z.H.O.U. Yu-Feng, *Progresses of theory on underground light dark matter direct detection-Cosmic-ray boosted dark matter and the Migdal effect*, *Sci. Sin. Phys. Mech. Astro.* **55** (2025) 111006 [INSPIRE].

[71] K.V. Berghaus, R. Essig and M.H. McDuffie, *The Migdal effect in Semiconductors for the Effective Field Theory of Dark Matter Direct Detection*, arXiv:2603.13052 [INSPIRE].

[72] F. Kahlhoefer and L. Su, *Probing Sub-GeV Dark Matter via Migdal Effect-Induced Electron Excitations*, arXiv:2604.26773 [INSPIRE].

[73] S. Nellen Mondragón, J. Pradler and M. Sholapurkar, *Adiabatic response in the Migdal Effect*, arXiv:2606.14845 [INSPIRE].

[74] LUX collaboration, *Results of a Search for Sub-GeV Dark Matter Using 2013 LUX Data*, *Phys. Rev. Lett.* **122** (2019) 131301 [arXiv:1811.11241] [INSPIRE].

[75] CDEX collaboration, *Constraints on Spin-Independent Nucleus Scattering with sub-GeV Weakly Interacting Massive Particle Dark Matter from the CDEX-1B Experiment at the China Jinping Underground Laboratory*, *Phys. Rev. Lett.* **123** (2019) 161301 [arXiv:1905.00354] [INSPIRE].

[76] XENON collaboration, *Search for Light Dark Matter Interactions Enhanced by the Migdal Effect or Bremsstrahlung in XENON1T*, *Phys. Rev. Lett.* **123** (2019) 241803 [arXiv:1907.12771] [INSPIRE].

[77] COSINE-100 collaboration, *Searching for low-mass dark matter via the Migdal effect in COSINE-100*, *Phys. Rev. D* **105** (2022) 042006 [arXiv:2110.05806] [INSPIRE].

[78] DarkSide collaboration, *Search for Dark-Matter-Nucleon Interactions via Migdal Effect with DarkSide-50*, *Phys. Rev. Lett.* **130** (2023) 101001 [arXiv:2207.11967] [INSPIRE].

[79] EDELWEISS collaboration, *Search for sub-GeV dark matter via the Migdal effect with an EDELWEISS germanium detector with NbSi transition-edge sensors*, *Phys. Rev. D* **106** (2022) 062004 [arXiv:2203.03993] [INSPIRE].

[80] SuperCDMS collaboration, *Search for low-mass dark matter via bremsstrahlung radiation and the Migdal effect in SuperCDMS*, *Phys. Rev. D* **107** (2023) 112013 [arXiv:2302.09115] [INSPIRE].

[81] PandaX collaboration, *Search for Dark-Matter-Nucleon Interactions with a Dark Mediator in PandaX-4T*, *Phys. Rev. Lett.* **131** (2023) 191002 [arXiv:2308.01540] [INSPIRE].

[82] D. Yi et al., *Direct observation of the Migdal effect induced by neutron bombardment*, *Nature* **649** (2026) 580 [INSPIRE].

[83] J. Xu et al., *Nuclear recoil Migdal effect in liquid xenon dark matter experiments*, *Appl. Phys. Lett.* **129** (2026) 134101 [arXiv:2606.03174] [INSPIRE].

JHEP11(2026)014

[84] MIGDAL collaboration, *The MIGDAL experiment: Measuring a rare atomic process to aid the search for dark matter*, *Astropart. Phys.* **151** (2023) 102853 [arXiv:2207.08284] [INSPIRE].

[85] K.D. Nakamura et al., *Detection capability of the Migdal effect for argon and xenon nuclei with position-sensitive gaseous detectors*, *PTEP* **2021** (2021) 013C01 [arXiv:2009.05939] [INSPIRE].

[86] Y. Lou and L. Wu, *Probing Dark Photons from Nuclear De-excitation in Reactor Neutrino Experiment*, arXiv:2606.08487 [INSPIRE].

[87] T. Gao and M. Pospelov, *Constraints on millicharged particles from nuclear γ-decays*, *Phys. Rev. D* **113** (2026) 115044 [arXiv:2507.17955] [INSPIRE].

[88] NEON collaboration, *First Direct Search for Light Dark Matter Using the NEON Experiment at a Nuclear Reactor*, *Phys. Rev. Lett.* **134** (2025) 021802 [arXiv:2407.16194] [INSPIRE].

[89] S.-F. Ge and I.M. Shoemaker, *Constraining Photon Portal Dark Matter with Texono and Coherent Data*, *JHEP* **11** (2018) 066 [arXiv:1710.10889] [INSPIRE].

[90] W. Dai et al., *Hunting for Axions in REactor neutrino COherent scattering Detection Experiment*, *Phys. Dark Univ.* **54** (2026) 102458 [arXiv:2509.01538] [INSPIRE].

[91] Y. Gong et al., *Constraints on axion-like particles with the silicon detector at a nuclear reactor*, *Sci. China Phys. Mech. Astron.* **69** (2026) 111013 [arXiv:2601.07448] [INSPIRE].

[92] TEXONO collaboration, *Constraints on millicharged particles with low threshold germanium detectors at Kuo-Sheng Reactor Neutrino Laboratory*, *Phys. Rev. D* **99** (2019) 032009 [arXiv:1808.02719] [INSPIRE].

[93] B. Kors and P. Nath, *A Stueckelberg extension of the standard model*, *Phys. Lett. B* **586** (2004) 366 [hep-ph/0402047] [INSPIRE].

[94] D. Feldman, Z. Liu and P. Nath, *The Stueckelberg Z-prime Extension with Kinetic Mixing and Milli-Charged Dark Matter From the Hidden Sector*, *Phys. Rev. D* **75** (2007) 115001 [hep-ph/0702123] [INSPIRE].

[95] D.E. Morrissey, D. Poland and K.M. Zurek, *Abelian Hidden Sectors at a GeV*, *JHEP* **07** (2009) 050 [arXiv:0904.2567] [INSPIRE].

[96] C. Pitrou and M. Pospelov, *QED corrections to Big-Bang nucleosynthesis reaction rates*, *Phys. Rev. C* **102** (2020) 015803 [arXiv:1904.07795] [INSPIRE].

[97] P. Talou and R. Vogt eds., *Nuclear Fission: Theories, Experiments and Applications*, Springer (2023) [DOI:10.1007/978-3-031-14545-2].

[98] TEXONO collaboration, *Production of electron neutrinos at nuclear power reactors and the prospects for neutrino physics*, *Phys. Rev. D* **72** (2005) 012006 [hep-ex/0502001] [INSPIRE].

[99] National Nuclear Data Center, *Evaluated Nuclear Structure Data File (ENSDF)*, https://www.nndc.bnl.gov/ensdf/ (2024).

[100] S.F. Mughabghab, *Atlas of Neutron Resonances: Resonance Parameters and Thermal Cross Sections, Z* = 1–100, 5th edition, Elsevier (2006).

[101] J. Lindhard, M. Scharff and H.E. Schiott, *Range concepts and heavy ion ranges*, *Mat. Fys. Medd. Dan. Vid. Selsk.* **33** (1963) 1.

[102] E. Stambulchik, *cFAC: a forked version of FAC*, https://github.com/fnevgeny/cfac.

[103] M.F. Gu, *The flexible atomic code*, *Can. J. Phys.* **86** (2008) 675.

[104] N.F. Bell et al., *Observing the Migdal effect from nuclear recoils of neutral particles with liquid xenon and argon detectors*, *Phys. Rev. D* **105** (2022) 096015 [arXiv:2112.08514] [INSPIRE].

JHEP11(2026)014

[105] C.E. Ekuma, M. Jarrell, J. Moreno and D. Bagayoko, *Re-examining the electronic structure of germanium: A first-principle study*, *Phys. Lett. A* **377** (2013) 2172.

[106] R.H. Helm, *Inelastic and Elastic Scattering of 187-Mev Electrons from Selected Even-Even Nuclei*, *Phys. Rev.* **104** (1956) 1466 [INSPIRE].

[107] M.A. Buen-Abad, R. Essig, D. McKeen and Y.-M. Zhong, *Cosmological constraints on dark matter interactions with ordinary matter*, *Phys. Rept.* **961** (2022) 1 [arXiv:2107.12377] [INSPIRE].

[108] SENSEI collaboration, *First Direct-Detection Results on Sub-GeV Dark Matter Using the SENSEI Detector at SNOLAB*, *Phys. Rev. Lett.* **134** (2025) 011804 [arXiv:2312.13342] [INSPIRE].

[109] C. Giovanetti, M. Lisanti, H. Liu and J.T. Ruderman, *Joint Cosmic Microwave Background and Big Bang Nucleosynthesis Constraints on Light Dark Sectors with Dark Radiation*, *Phys. Rev. Lett.* **129** (2022) 021302 [arXiv:2109.03246] [INSPIRE].

[110] S.-F. Ge, J. Sheng, C. Xia and C.-Y. Xing, *Nuclear production and analytic attenuation of energetic MeV solar dark matter*, *Phys. Lett. B* **880** (2026) 140758 [arXiv:2408.12448] [INSPIRE].

[111] J.H. Chang, R. Essig and A. Reinert, *Light(ly)-coupled Dark Matter in the keV Range: Freeze-In and Constraints*, *JHEP* **03** (2021) 141 [arXiv:1911.03389] [INSPIRE].

[112] J.H. Chang, R. Essig and S.D. McDermott, *Supernova 1987A Constraints on Sub-GeV Dark Sectors, Millicharged Particles, the QCD Axion, and an Axion-like Particle*, *JHEP* **09** (2018) 051 [arXiv:1803.00993] [INSPIRE].

[113] D.F.G. Fiorillo and E. Vitagliano, *Self-Interacting Dark Sectors in Supernovae Can Behave as a Relativistic Fluid*, *Phys. Rev. Lett.* **133** (2024) 251004 [arXiv:2404.07714] [INSPIRE].

JHEP11(2026)014